Energy Conversion and Management 223 (2020) 113293

Contents lists available at ScienceDirect

Energy Conversion and Management

journal homepage: www.elsevier.com/locate/enconman

Energy and exergy analysis of a new cogeneration system based on an organic Rankine cycle and absorption heat pump in the coal-fired power plant

Hongsheng Zhang *, Yifeng Liu, Xingang Liu, Chenghong Duan

College of Mechanical and Electrical Engineering, Beijing University of Chemical Technology, Beijing 100029, PR China

ARTICLE INFO

Keywords:
Energy and exergy analysis
Organic Rankine cycle
Absorption heat pump
Cogeneration system
Waste heat recycle

ABSTRACT

A new cogeneration system based on ORC (organic Rankine cycle) and AHP (absorption heat pump) is presented to achieve the dual effects of improving power output and heating capacity in a coal-fired power plant. The heat source for heating is firstly led into the ORC to generate power, and then is led into the AHP as the driving heat source to recycle waste heat from exhausted steam of the ST (steam turbine) when the energy grade is reduced to a level that matches with the heating energy grade. On the basis of the thermodynamic first and second law, focusing on 135 MW coal-fired power plant, the energy and exergy analyses of traditional cogeneration system and new cogeneration system with ORC and AHP have been completed. Compared to the traditional cogeneration system, the power output and heating capacity are respectively increased by 1.47 MW and 32,106.64 kW when the flow rate of heating extraction steam is 40 kg/s. The integral thermal and exergy efficiencies are improved by 9.38% and 1.71%. Moreover, the coal consumption decrement for power generation and heat-supplying both augments with increasing heating extraction flow rate and decreasing load. The new presented scheme can not only reduce the irreversible loss of the cogeneration system but also save coal consumption.

1. Introduction

With increasingly serious energy crisis and environmental pollution caused by fossil fuels, the energy conservation and emission reduction are being paid more and more attention [1]. The clean renewable energy, such as solar, geothermal, biomass, etc., are considered as promising alternative energy resources in the future [2]. However, at present, the renewable energy cannot be widely used due to some problems, including technology problem, high cost, etc [3]. In this case, energy conservation measure for fossil energy is an important way to alleviate the energy shortage and environmental pollution at present [4]. Especially for China dominated by coal, the coal-fired power generation is the main form of electricity production, which is an important industry of energy conservation and emission reduction [5].

Cogeneration based on energy cascade utilization has been recognized as an efficient energy-saving mode due to the advantages of high comprehensive energy utilization efficiency and low pollution emission around the world [6]. At present, it has become the main heat supplying form in China. The energy utilization efficiency has been improved to some extent, there is still some energy waste in the thermal power plants. In particular, the waste heat of low-temperature exhausted steam of the units is usually discharged into the environment due to the low temperature, which leads to not only energy dissipation but also heat pollution [7]. The quality of this part of energy is low, but the amount is huge with a large recovery potential [8]. The development of energy-saving technology, such as organic Rankine cycle, heat pump technology, electrical turbo-compounding, etc, makes it possible to recover the low-temperature waste heat [9]. Among them, the absorption heat pump is an effective way to recover the waste heat of low-temperature exhausted steam from steam turbine.

In order to develop the technology of waste heat recovery by absorption heat pumps, many studies have been carried out in recent years. Li et al. [10] coupled an absorption heat pump to a solar tower power plant to recover the waste heat of exhausted steam from steam turbine to enhance the efficiency of solar energy utilization. The results demonstrate that the waste heat of 914 MJ is obtained and the efficiency of solar energy utilization is improved by 4.55%. In the following study, they used an absorption heat pump to recycle the condensation waste heat of exhaust steam from steam turbine in a solar thermal power plant. The thermal efficiency can be up to 80.5% when all the condensation waste heat is recovered by the absorption heat pump. The energy and

* Corresponding author.
E-mail address: zhangguotang@aliyun.com (H. Zhang).

https://doi.org/10.1016/j.enconman.2020.113293
Received 1 June 2020; Received in revised form 31 July 2020; Accepted 1 August 2020
Available online 10 August 2020

Nomenclature

Abbreviations

ORC	organic Rankine cycle
AHP	Absorption heat pump
ST	Steam turbine
HPT	High pressure turbine
IPT	Intermediate pressure turbine
LPT	Low pressure turbine
ACC	Air cooling condenser
RS	Regenerative system
CP	Condensate pump
HPFWH	High pressure feed-water heater
LPFWH	Low pressure feed-water heater
HHN	Heater for heating network
HC	Heat consumer
CWCP	Cooling water circulating pump
COP	Coefficient of performance
VMP	Working medium pump
SHE	Solution heat exchanger
LHV	Low calorific value of standard coal
THA	Turbine heat acceptance

Variables

h	Steam specific enthalpy (kJ/kg)
q	Heat released by per kg extracted steam (kJ/kg)
τ	Enthalpy increment of per kg feed water (kJ/kg)
γ	Heat released by per kg drain (kJ/kg)
$\bar{t}$	Water specific enthalpy (kJ/kg)
G	Mass flow rate (kg/s)
η	Efficiency
Pe	Power (MW)
Q	Energy (kW)
a, b, c	Mass concentration of lithium bromide
m	Standard coal consumption (kg/s)
Ex	Exergy (kW)
W	Work (kJ)

Subscripts

j	Extraction stage j of the turbine
fw	Feed water
abs	Absorber
con	Condenser
gen	Generator
eva	Evaporator
ps	Live Steam
rs	Reheated Steam
bl	Boiler
p	Power
h	Heating
in	Inlet
out	Outlet
r	Refrigerant
ss	Strong solution
sp	Solution pump
$lths$	Low temperature heat source
hcw	Heating condensate water
ws	Weak solution
th	Thermal
ex	Exergy

exergy efficiency is respectively improved by 0.27% and 0.29%, and heating cost is greatly reduced [11]. Sun et al. [12] put forward a new district heating system in which the absorption heat pump and ejector heat exchangers are used to recover waste heat of exhaust steam from the steam turbine. The results show that the extraction steam consumption is reduced by 41.4%, and heating capacity is increased by 66.7% in the new heating system. Zhang et al. [13] proposed a novel cogeneration system based on an absorption heat pump to recover waste heat of exhaust steam from a coal-fired power plant. The results indicate that the coal consumption rate is decreased by 8.74–20.73 g/kWh, overall energy efficiency and exergy efficiency are respectively improved by 1.15%-1.91% and 1.19%-2.03% at different loads. In subsequent studies, they presented a new air-cooled gas-steam power plant equipped an absorption heat pump to recover waste heat from exhausted steam to replace a conventional water-cooling gas-steam power plant to save energy and water. The energy-saving effect of waste heat recovery by absorption heat pump can make up for the performance degradation caused by air cooling transformation [14]. Xu et al. [15] adopted large scale absorption heat pumps to recycle condensed waste heat of exhaust steam to supply heating and discussed the benefits from the theoretical analysis and practical test. The result shows that the 1.27PJ waste heat can be obtained, the consumption water and CO_2 emission can be significantly reduced. Li et al. [16] adopted an absorption heat pump to recover condensation waste heat from two 300 MW water-cooled steam turbines and compared with conventional heating system and high-backpressure heating system. The equivalent electricity for heating is reduced by 11.1%–29.4%, the overall exergy efficiency is improved by 6.1%–14.1%, and the heating cost is reduced by 8.7%–23.9%.

As mentioned above, the significant energy-saving effect of AHP (absorption heat pump) that is used to recycle waste heat from exhausted steam of the steam turbine has been verified by many researches. However, the existing extraction steam in the regenerative system is often used as the driving heat source of AHP, so the fact that the energy grade of driving heat source of AHP is much higher than that of heat required by heat consumer to result in the mismatch between heating supply side and heating receiving side is usually ignored in the coal-fired power plants.

Organic Rankine cycle (ORC) is an efficient method to generate power by medium- and low-temperature heat due to using low-boiling point organics as working medium [17]. The study about organic Rankine cycle is an important topic. Campos et al. [18] carried out thermoeconomic optimization on the organic Rankine cycle applied to recycle the waste heat of flue gas from a microturbine. The results show that the power output is increased by 14.1 kWe and electric efficiency is improved by 4.2%. Linnemann et al. [19] designed a power plant equipped with two cascaded organic Rankine cycles driven by the exhausted gas from a cogeneration power plant. The design, working fluid selection and initial tests were completed to obtain the max plant efficiency. Moreira et al. [20] analyzed thermodynamic performance of the organic Rankine cycles with and without regenerative form to recover waste heat of the cement factories. The generated power is increased by 4,000–9,000 kW and the carbon dioxide emission is reduced by 221,069 kg per year. Bălănescu and Homutescu [21] employed an organic Rankine cycle to recover the waste heat from flue gas of a gas turbine combined cycle power plant. The results indicate that the additional power is obtained and the efficiency is improved by 1.1% around. Therefore, additional power can be obtained from ORC driven by medium- and low-temperature heat.

A novel cogeneration scheme in which the ORC and AHP are simultaneously applied in the heating system is proposed to achieve the dual effects of improving power output and heating capacity in a coal-fired power plant in the paper. The high quality extraction steam for heating is firstly considered as driving heat source of ORC to generate

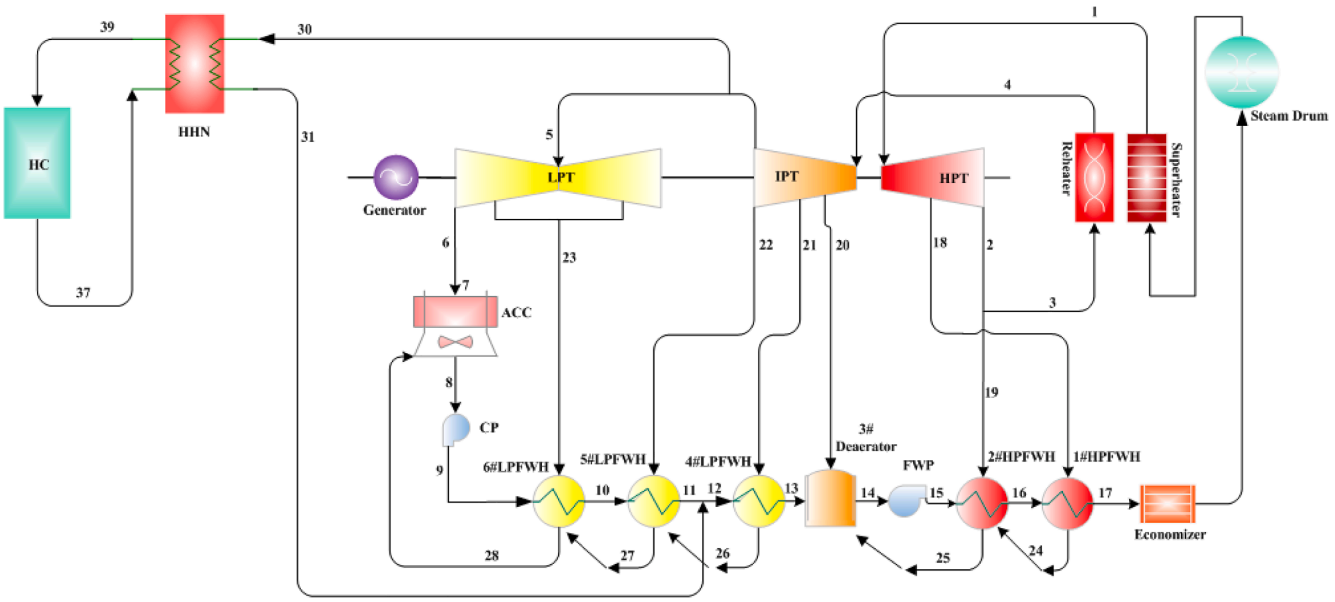

Fig. 1. Flow chart of the traditional cogeneration system.

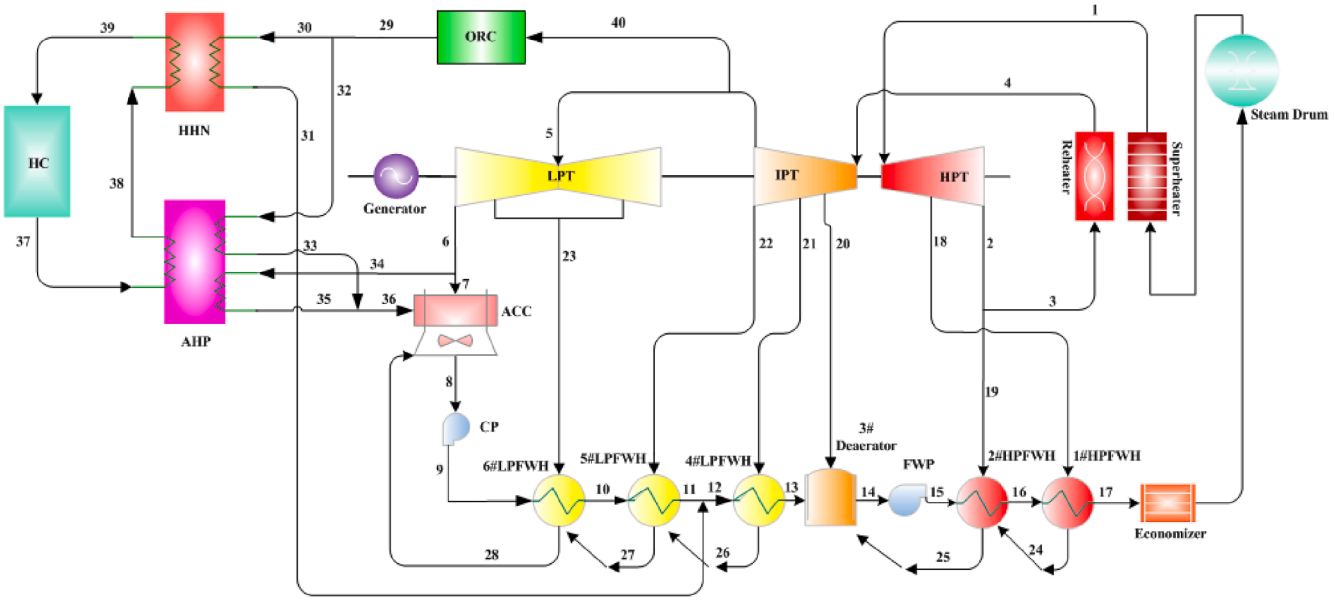

Fig. 2. Flow chart of the new cogeneration system with ORC and AHP.

power, and then as heat source for heating when its energy grade is reduced to a level that matches with the heating energy grade. Therefore, the deep energy cascade utilization can be realized. It is more conductive to reduce the irreversible loss between heating supply side and heating receiving side. The scheme is more in line with the principle of energy cascade utilization, that is, high grade heat energy is used to generate power and low-grade heat energy is used to supply heating. Based on energy and exergy analysis methods, taking a 135 MW coal-fired unit in northern China as a case study, the performance analyses of the traditional cogeneration system and the novel cogeneration system have been carried out. The performance changing laws have been revealed before and after transformation. The energy and exergy indicator changes have been quantitatively displayed after the transformation. FORTRAN (Formula Translation) is adopted as simulation software in the paper.

2. System description

The flow charts of traditional cogeneration system and the new cogeneration system with ORC and AHP are respectively illustrated in Figs. 1 and 2. The steam turbine (ST) consists of a HPT (High-pressure turbine), IPT (Intermediate-pressure turbine) and LPT (Low-pressure turbine). The regenerative system (RS) comprises two high pressure feed-water heaters (HPFWH), a deaerator and three low pressure feed-water heaters (LPFWH).

2.1. Traditional cogeneration system

As displayed in Fig. 1, only a HHN (Heater for heating network) is adopted to heat the backwater from heat consumer (HC) in the traditional cogeneration system. The heat source (No. 30) for heating is derived from the fifth stage extraction steam of ST. The condensation

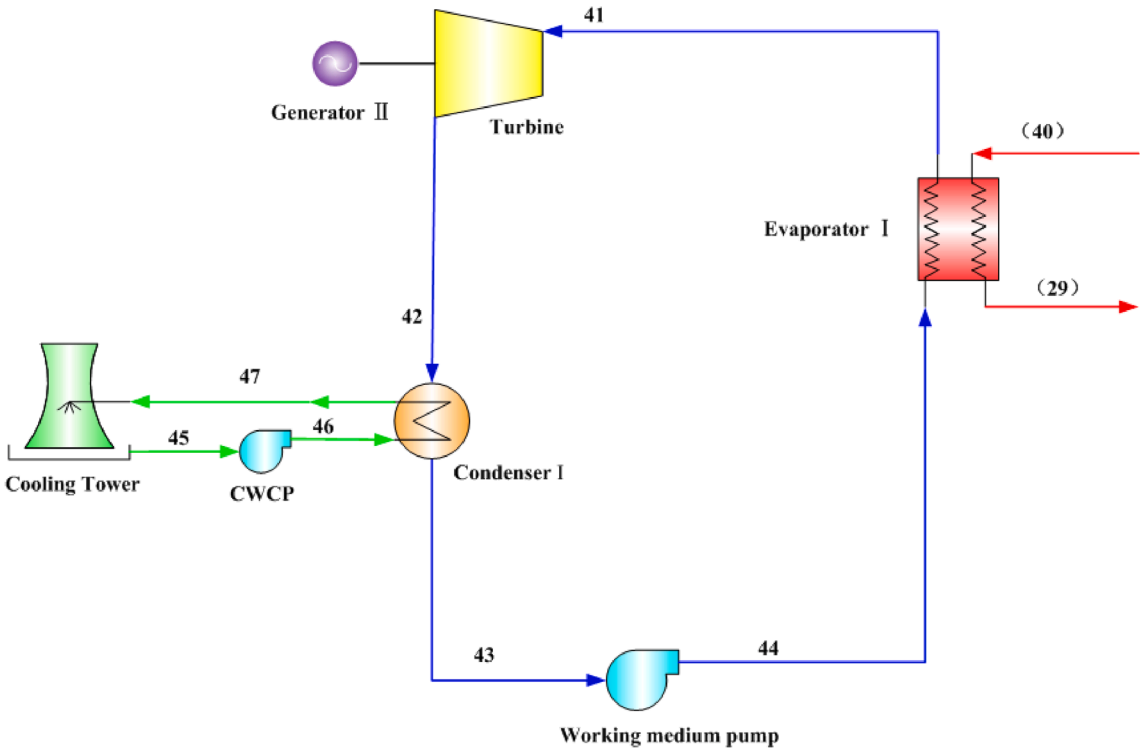

Fig. 3. Schematic diagram of ORC.

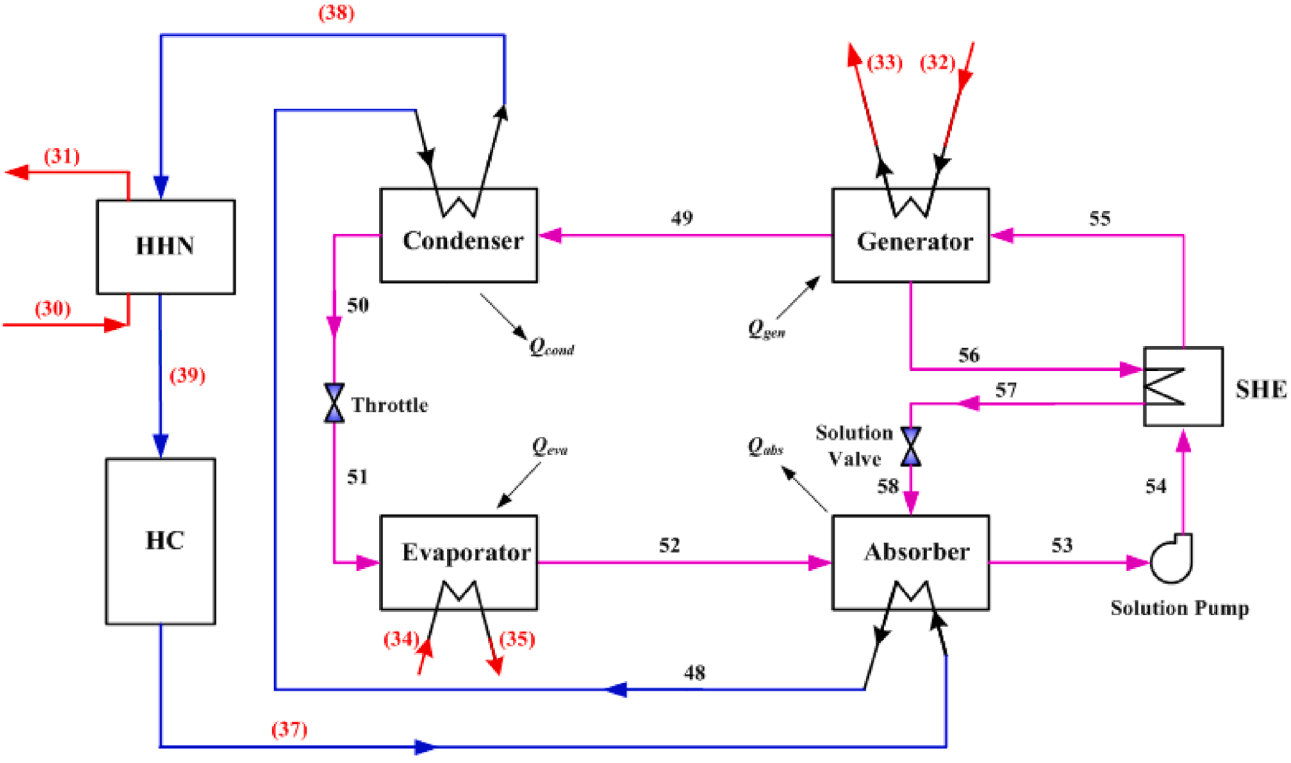

Fig. 4. Schematic diagram of AHP-HHN.

water (No. 31) is led into the fourth LPFWH to return into the cycle.

2.2. New cogeneration system with ORC and AHP

The flow chart of the new cogeneration system is shown in Fig. 2. An ORC (organic Rankine cycle) and an AHP (Absorption heat pump) are added in the new cogeneration system. The heat source for heating still comes from the fifth stage extraction steam. The heat source for heating is firstly led into the ORC to generate power (No. 40), and then is led into the AHP as the driving heat source (No. 32) when the energy grade is

Table 1
Main design parameters.

Parameter	Value
Ambient temperature (°C)	10.00
Ambient pressure (kPa)	100.00
COP of AHP	1.73
Boiler efficiency	0.92
Generator efficiency	0.99
Low calorific value of standard coal (kJ/kg)	29,308.00
Temperature at outlet of evaporator of ORC (°C)	190.00
Condensate pressure of ORC (kPa)	112.00
Temperature of driving heat source of AHP (°C)	150.00
Backwater temperature (°C)	55.00
Backwater temperature at outlet of AHP (°C)	75.00
Backwater temperature at outlet of HHN (°C)	85.00

reduced to a level that matches the heating energy grade. The low-temperature heat source (No. 34) is derived from exhausted steam of steam turbine. The stream No. 34 is a part of the exhausted steam from ST. It was supposed to go into the ACC (Air cooling condenser) to be condensed and release heat to the atmosphere, but it is recovered as low-temperature heat source of AHP to recover waste heat and increase heating capacity in the new cogeneration system. The condensation water of driving and low-temperature heat source (No. 33 and 35) is led into the ACC to be further condensed and eventually return into the cycle. The backwater (No. 37) is firstly heated by AHP (No. 38), and then is heated to the required temperature by HHN (No. 39), instead of being heated only by HHN in the traditional heating system. The combined application of ORC and AHP can not only increase the power generation, but also recover the waste heat of exhausted steam for heating to increase the heating capacity at the same flow rate of extraction steam for heating. Moreover, the energy grade difference between the heat consumer and heating network can be reduced in the new cogeneration system, which reduces the irreversible loss and improves the energy utilization efficiency of the system.

The schematic diagram of ORC is shown in Fig. 3. The driving heat source of ORC comes from the fifth stage extraction steam whose teamperature ranges from 225 to 235 °C at three design conditions. The R141b is chosen as an organic working medium in the ORC [22]. The schematic diagram of AHP-HHN is shown in Fig. 4. The backwater from HC is heated from 55 °C to 75 °C by AHP and then is heated to 85 °C by HHN. The "heat increasing type" heat pump using lithium bromide and water as the working pairs is adopted [23]. The single-effect absorption heat pump is employed in the paper. The main design parameters are displayed in Table 1.

3. Thermodynamic model and assessment indicators

The energy grade difference between the heating supply side and heating receiving side of the heating system can not only be reduced but also recover a part of waste heat of exhausted steam from ST for heating in the new cogeneration system. The following assumptions are adopted in establishing the thermodynamic model:

(a) The original state parameters of the system remain unchanged before and after the transformation.
(b) The heat losses of pipelines and equipments are ignored as well as the pressure drop.
(c) The kinetic and potential energy are ignored.
(d) The outlet of evaporator and condenser of ORC are saturated.
(e) The system is operated in a steady state.

3.1. Model of regenerative system

The RS (regenerative system) incorporates two types of feed-water heaters. One is a closed heater and the other is an open feed-water heater. The feed water and extraction steam are kept separate in heat exchange process in a closed heater, while the both are allowed to be mixed in an open feed-water heater. The schematic diagrams of two types of feed-water heaters are exhibited in Fig. 5.

For closed feed-water heater exhibited in Fig. 5(a), the energy balance equation can be expressed:

$$\tau_j = \bar{t}_j - \bar{t}_{j-1} \tag{1}$$

$$q_j = h_j - \bar{t}_{sj} \tag{2}$$

$$\gamma_j = \bar{t}_{s(j+1)} - \bar{t}_{sj} \tag{3}$$

For the open feed-water heater exhibited in Fig. 5(b), the energy balance equation can be expressed:

$$\tau_j = \bar{t}_j - \bar{t}_{j-1} \tag{4}$$

$$q_j = h_j - \bar{t}_{j-1} \tag{5}$$

$$\gamma_j = \bar{t}_{s(j+1)} - \bar{t}_{j-1} \tag{6}$$

The flow rates of extracted stages can be calculated by following energy-efficiency distribution matrix equation [24]:

$$\begin{bmatrix} q_1 & & & & & \\ \gamma_1 & q_2 & & & & \\ \gamma_3 & \gamma_3 & q_3 & & & \\ \tau_4 & \tau_4 & \tau_4 & q_4 & & \\ \tau_5 & \tau_5 & \tau_5 & \gamma_5 & q_5 & \\ \tau_6 & \tau_6 & \tau_6 & \gamma_6 & \gamma_6 & q_6 \end{bmatrix} \begin{bmatrix} G_1 \\ G_2 \\ G_3 \\ G_4 \\ G_5 \\ G_6 \end{bmatrix} = \begin{bmatrix} \tau_1 & & & & & \\ & \tau_2 & & & & \\ & & \tau_3 & & & \\ & & & \tau_4 & & \\ & & & & \tau_5 & \\ & & & & & \tau_6 \end{bmatrix} \begin{bmatrix} G_{fw} \\ G_{fw} \\ G_{fw} \\ G_{fw} \\ G_{fw} \\ G_{fw} \end{bmatrix} \tag{7}$$

where i denotes extracted stage; G_i denotes flow rate of i extracted steam kg/s; G_{fw} denotes flow rate of feed water, kg/s.

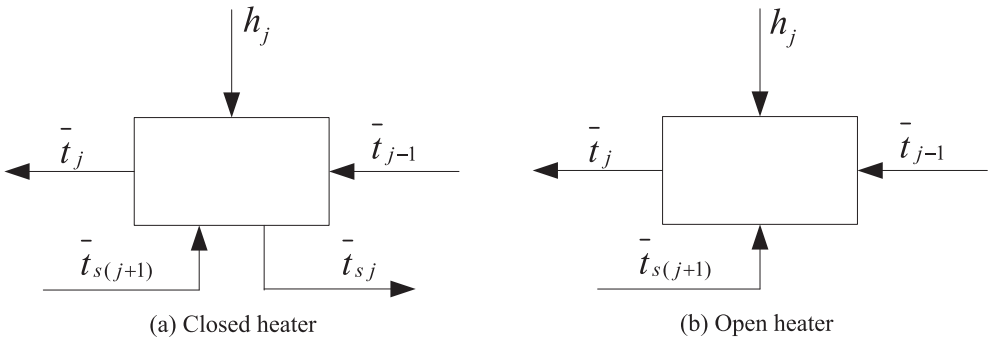

Fig. 5. Schematic diagrams of feed-water heaters.

3.2. Model of ORC

The specific enthalpy at outlet of the turbine can be expressed as following [25]:

$$h_{42} = h_{41} - (h_{41} - h_{42s}) \times \eta_t \tag{8}$$

where h_{41} and h_{42} respectively denote specific enthalpy at inlet and outlet of the turbine, kJ/kg; h_{42s} denotes isentropic specific enthalpy at outlet of the turbine kJ/kg; η_t denotes relative internal efficiency of the turbine, %.

The generation power of the turbine:

$$Pe_t = G_{gz} \times (h_{41} - h_{42}) \times \eta_g \tag{9}$$

where Pe_t denotes generation power of the turbine, kW; G_{gz} denotes flow rate of organic working medium, kg/s; η_g denotes the generator efficiency, %.

The heat released in the condenser I can be expressed:

$$Q_{condenserI} = G_{gz} \times (h_{42} - h_{43}) \tag{10}$$

where h_{43} denotes specific enthalpy at outlet of condenser I, kJ/kg.

The electrical power consumed by the pump can be expressed [26]:

$$Pe_{wmp} = G_{gz} \times (h_{44} - h_{43})/\eta_{wmp} \tag{11}$$

$$Pe_{CWCP} = G_{cwcp} \times (h_{46} - h_{45})/\eta_{CWCP} \tag{12}$$

where Pe_{wmp} and Pe_{CWCP} respectively denotes the electrical power consumed by WMP (Working medium pump) and CWCP (Cooling water circulating pump), kW; h_{44} denotes specific enthalpy at outlet of WMP, kJ/kg; h_{45} and h_{46} respectively denote specific enthalpy at inlet and outlet of CWCP, kJ/kg; η_{wmp} and η_{CWCP} denotes the efficiency of WMP and CWCP, %.

The net generating power of ORC:

$$Pe_{t,\text{net}} = Pe_t - Pe_{wmp} - Pe_{CWCP} \tag{13}$$

The exchanged heat of organic working medium in the Evaporator I can be expressed:

$$Q_{evaporatorI} = G_{gz} \times (h_{41} - h_{44}) \tag{14}$$

The thermal and exergy efficiency of ORC can be expressed:

$$\eta_{th-ORC} = \frac{Pe_{t,net}}{Q_{condenserI}} \times 100 \tag{15}$$

$$\eta_{ex-ORC} = \frac{Pe_{t,net}}{Ex_{40} - Ex_{29}} \times 100 \tag{16}$$

where η_{th-ORC} and η_{ex-ORC} respectively denotes the thermal and exergy efficiency of ORC, %;Ex_{40} and Ex_{29} denotes the exergy of inlet and outlet of heat source of ORC, kW.

3.3. Model of AHP-HHN system

The heating system is consists of an AHP and a HHN shown in Fig. 4. The model of each component can be expressed as follows:

Generator (No. 45 → 49, 46) and (No. 32 → 33):

The driving heat source provides energy to the working medium pair of lithium bromide solution in the generator. The equations below can be given on the basis of energy and quality conservation:

$$Q_{gen} = G_{dhs}(h_{32} - h_{33}) \tag{17}$$

$$G_{dhs}(h_{32} - h_{33}) = G_r h_{49} + G_{ss} h_{56} - G_{ws} h_{55} \tag{18}$$

$$G_{ws} = G_{ss} + G_r \tag{19}$$

$$G_{ws} a = G_{ss} b + G_r c \tag{20}$$

Condenser (No. 49 → 50) and (No. 48 → 38):

The refrigerant releases heat to the backwater in the condenser. The equations below can be given on the basis of energy and quality conservation:

$$Q_{cond} = G_r(h_{49} - h_{50}) \tag{21}$$

$$G_r(h_{49} - h_{50}) = G_{hcw}(h_{38} - h_{48}) \tag{22}$$

Throttle (No. 50 → 51):

The throttle is adopted to decrease the pressure of the refrigerant into the evaporator. It can be considered an adiabatic process due to no heat exchange. The equations below can be given on the basis of energy conservation:

$$h_{50} = h_{51} \tag{23}$$

Evaporator (No. 51 → 52) and (No. 34 → 35):

The exhausted steam from ST as low-temperature heat source provides heat to the solution in the evaporator. The equations below can be given on the basis of energy and quality conservation:

$$Q_{eva} = G_r(h_{52} - h_{51}) \tag{24}$$

$$G_r(h_{52} - h_{51}) = G_{lths}(h_{34} - h_{35}) \tag{25}$$

Absorber (No. 52, 58 → 53) and (No.37 → 48):

The low pressure refrigerant is absorbed by concentrated solution to release heat that is provided to the backwater in the absorber. The equations below can be given on the basis of energy and quality conservation:

$$Q_{abs} = G_r h_{52} + G_{ss} h_{58} - G_{ws} h_{53} \tag{26}$$

$$G_r h_{52} + G_{ss} h_{58} - G_{ws} h_{53} = G_{hcw}(h_{48} - h_{37}) \tag{27}$$

$$G_r + G_{ss} = G_{ws} \tag{28}$$

$$G_r c + G_{ss} b = G_{ws} a \tag{29}$$

Solution pump (No. 53 → 54):

The solution pump is adopted to raise the strong solution pressure at outlet of the absorber. The electrical power consumed by solution pump can be expressed:

$$Pe_{sp} = G_{ws}(h_{54} - h_{53})/\eta_{sp} \tag{30}$$

Solution heat exchanger (No. 54 → 55) and (56 → 57):

The strong solution into generator is preheated by solution heat exchanger (SHE). The equations below can be given on the basis of energy and quality conservation:

$$G_{ws}(h_{55} - h_{54}) = G_{ss}(h_{56} - h_{57}) \tag{31}$$

Solution valve (No. 57 → 58):

The pressure of strong solution into the absorber is reduced by solution valve. It can be considered an adiabatic process due to no heat exchange. The equations below can be given on the basis of energy conservation:

$$h_{57} = h_{58} \tag{32}$$

Heater for heating network (No. 38 → 39) and (No. 30 → 31):

The backwater is heated to the required temperature by HHN (Heater for heating network). The equations below can be given on the basis of energy conservation:

$$G_{hcw}(h_{39} - h_{38}) = G_{hhes}(h_{30} - h_{31}) \tag{33}$$

Heat consumer (No. 39 → 37):

The heat consumer (HC) obtains heat energy from the heating network. The equations below can be given on the basis of energy

conservation:

$$Q_{consumer} = G_{hcw}(h_{39} - h_{37}) \tag{34}$$

Determination of COP

COP (Coefficient of performance) [27] is an important evaluation indicator for absorption heat pump. It can be calculated as follows:

$$COP = \frac{Q_{abs} + Q_{cond}}{Q_{gen}} \tag{35}$$

where Q_{abs} and Q_{cond} denotes heat exchange in absorber and condenser, kW; Q_{gen} denotes heat provided by the driving heat source, kW. They have been displayed in Fig. 4. The COP of single-effect AHP with lithium bromide solution as working medium is generally 1.65–1.85 [28]. The COP of hot water single-effect absorption heat pumps varies between 1.5 and 1.8 when the temperature of driving heat source is 90–130 °C and the temperature of low-grade heat source is 15–40 °C [29]. Abrahamsson et al. [30] conducted a simulation for the absorption heat pump with lithium bromide solution, and the value for COP is 1.80 when the temperature of driving heat source is 139 °C. The COP of AHP calculated in this paper is 1.73 listed in Table 1.

3.4. Assessment indicator

Power output, standard coal consumption, integral thermal efficiency, exergy loss and integral exergy efficiency are chosen as important assessment indicators in the traditional cogeneration system and new cogeneration system with ORC and AHP.

3.4.1. Power output

Power output of the steam turbine can be expressed as following:

$$\begin{aligned} Pe_{ST} = {} & (G_{ps} \times (h_{ps} - h_1) + \sum_{m=2}^{n_1} \left(G_{ps} - \sum_{i=1}^{m-1} G_i \right)(h_{m-1} - h_m) + \\ & G_{rs} \times (h_{rs} - h_{n_1+1}) + \sum_{m=n_1+2}^{n_1+n_2+1} \left(G_{rs} - \sum_{i=n_1+1}^{m-1} G_i \right)(h_{m-1} - h_m)) \times \eta_g \end{aligned} \tag{36}$$

where Pe_{ST} denotes power output of steam turbine, kW; G_{ps}, G_i and G_{rs} respectively denotes flow rates of the primary steam, i stage extraction steam and reheated steam, kg/s; h_{ps}, h_{rs} and h_m respectively denotes specific enthalpy of the primary steam, reheated steam and m stage extraction steam, kJ/kg; n_1, n_2 denotes extraction steam stage numbers before and after reheating; $n_1 + n_2 + 1$ denotes the exhausted steam stage.

Integral power output of the system can be expressed as follows:

$$Pe_{integral} = Pe_{ST} + Pe_{t,net} \tag{37}$$

3.4.2. Heating capacity

The heating capacity of the system can be expressed as follows:

$$Q_{heating} = G_{32} \times (h_{32} - h_{33}) + G_{34} \times (h_{34} - h_{35}) + G_{30} \times (h_{30} - h_{31}) \tag{38}$$

where $Q_{heating}$ denotes heating capacity of the system, kW; G_{34}, G_{32} and G_{30} respectively denotes flow rates of stream No. 34, 32, 30, kg/s.

3.4.3. Coal consumption for power generation and heat-supplying

The overall standard coal consumption mass flow rate in the cogeneration system is given:

$$m_c = \left(G_{ps} \times \left(h_{ps} - h_{fw}\right) + G_{rs} \times (h_{rs} - h_{crs})\right) / (\eta_{bl} \times LHV_{coal}) \tag{39}$$

where m_c denotes overall standard coal consumption mass flow rate, kg/s; h_{fw} and h_{crs} respectively denote specific enthalpy of primary feed water and cold reheated steam, kJ/kg; LHV_{coal} denotes low calorific value for standard coal, kJ/kg; η_{bl} denotes boiler efficiency, %.

The standard coal consumption mass flow rates for heat supplying and power generation in the cogeneration system are given:

$$m_{c,h} = \alpha_{h0} \times m_c \tag{40}$$

$$m_{c,p} = (1 - \alpha_{h0}) \times m_c \tag{41}$$

where $m_{c,h}$ and $m_{c,p}$ respectively denote standard coal consumption mass flow rates for heat supplying and power generation, kg/s; α_{h0} denotes modified heating ratio that is obtained simultaneously considering both the quality and quantity of heating energy.

$$\alpha_{h0} = \frac{\alpha_h}{1 + \lambda \alpha_h} \tag{42}$$

where α_h denotes heating ratio; λ denotes correction factor that is related to the units; The value for λ is approximately chosen as 0.251 [31].

$$\alpha_h = Q_{heating} / Q_{integral} \tag{43}$$

where $Q_{integral}$ denotes integral energy input into the cogeneration system, kW.

$$Q_{integral} = \left(G_{ps} \times \left(h_{ps} - h_{fw}\right) + G_{rs} \times (h_{rs} - h_{crs})\right) / \eta_{bl} \tag{44}$$

The coal consumptions for power generation and heating supply are given:

$$m_{cr,p} = \frac{3.6 \times 10^6 \times m_{c,p}}{P_{integral}} \tag{45}$$

$$m_{cr,h} = \frac{10^6 \times m_{c,h}}{Q_{integral}} \tag{46}$$

where $m_{cr,p}$ and $m_{cr,h}$ respectively denotes coal consumptions for power generation and heating supply, g/kWh, kg/GJ.

3.5. Exergy analysis model

The following mass conservation equation, energy conservation equation, entropy equation and exergy balance equation are involved to complete an exergy analysis [32].

$$\sum_i (\delta m_i)_{in} = \sum_j (\delta m_j)_{out} \tag{47}$$

$$\delta Q = \sum_j (\delta m_j \times h_j)_{out} - \sum_i (\delta m_i \times h_i)_{in} + \delta W \tag{48}$$

$$\sum_i \delta m_i s_i - \sum_j \delta m_j s_j + \sum_l \frac{\delta Q_l}{T_{r,l}} + \delta S_g = 0 \tag{49}$$

$$\sum Ex_{in} + \sum Ex_Q - \sum Ex_{out} - W = \sum Ex_{loss} \tag{50}$$

where, m_i and m_j denotes flow rate entering into and out of the system; h_i, h_j, s_i and s_j respectively denotes corresponding specific enthalpy and entropy; W denotes the work done by the system; Ex_{in}, Ex_{out}, Ex_Q and Ex_{loss} respectively denotes the exergy at the inlet, exergy at the outlet, exergy contained in exchanged heat and exergy loss caused by irreversibility.

3.6. Integral efficiency

The integral thermal and exergy efficiencies of the cogeneration system are given as following [33]:

$$\eta_{th} = \frac{P_{integral} + Q_{heating}}{Q_{integral}} \tag{51}$$

Table 2
Thermodynamic parameters at 100%THA load when the flow rate of heating extraction steam is 40 kg/s.

Stream no.	Flow rate (kg/s)	Pressure (kPa)	Temperature (°C)	Specific enthalpy (kJ/kg)	Specific entropy (kJ/(kg·K))	Specific exergy (kJ/kg)
1	118.92	13240.00	535.00	3429.15	6.55	1575.40
2	113.02	2598.00	319.80	3054.37	6.71	1156.21
3	101.08	2598.00	319.80	3054.37	6.71	1156.21
4	101.08	2338.00	535.00	3542.25	7.46	1431.66
5	48.67 (48.85)	223.00	232.70	2935.65	7.59	786.94
6	44.38 (45.85)	15.00	54.00	2519.70	7.77	321.18
7	27.96 (45.85)	15.00	54.00	2519.70	7.77	321.18
8	79.14 (57.92)	15.00	54.00	226.06	0.76	12.88
9	79.14 (57.92)	1874.00	54.20	228.48	0.76	14.84
10	79.14 (57.92)	1794.00	87.80	369.06	1.17	39.60
11	79.14 (57.92)	1739.00	125.17 (136.96)	526.82 (577.07)	1.58 (1.71)	79.57 (94.62)
12	97.92	1724.00	119.00	500.62	1.52	72.13
13	97.92	1654.00	143.10	603.32	1.77	102.81
14	118.92	1463.00	163.40	690.82	1.98	132.06
15	118.92	16000.00	166.10	710.92	1.99	149.52
16	118.92	16000.00	221.40	954.15	2.51	245.15
17	118.92	16000.00	243.40	1055.15	2.71	289.57
18	5.89	3604.00	361.00	3129.10	6.69	1236.62
19	11.94	2598.00	319.80	3054.37	6.71	1156.21
20	3.16	708.00	369.40	3204.65	7.53	1072.23
21	4.15	427.00	305.70	3078.15	7.56	939.04
22	5.10 (4.91)	223.00	232.70	2935.65	7.59	786.94
23	4.28 (3.01)	76.00	133.20	2745.22	7.66	575.63
24	5.89	3496.20	242.50	1049.48	2.72	278.60
25	17.84	873.70	174.10	737.19	2.08	148.30
26	4.15	405.40	144.10	606.82	178	103.02
27	9.25 (9.06)	212.2	122.10	512.72	1.55	74.37
28	13.53 (12.07)	72.30	90.80	380.33	1.20	40.67
29	40.00 (0.00)	223.00 (0.00)	150.00 (0.00)	2767.31 (0.00)	7.23 (0.00)	721.54 (0.00)
30	18.78 (40.00)	223.00	150.00 (232.70)	2767.31 (2935.65)	7.23 (7.59)	721.54 (786.94)
31	18.78 (40.00)	78.600	93.00	389.59	1.23	42.76
32	21.22 (0.00)	223.00 (0.00)	150.00 (0.00)	2767.31 (0.00)	7.23 (0.00)	721.54 (0.00)
33	21.22 (0.00)	80.00 (0.00)	80.00 (0.00)	334.97 (0.00)	1.08 (0.00)	31.14 (0.00)
34	16.43 (0.00)	15.00 (0.00)	54.00 (0.00)	2519.70 (0.00)	7.77 (0.00)	321.18 (0.00)
35	16.43 (0.00)	15.00 (0.00)	54.00 (0.00)	226.06 (0.00)	0.76 (0.00)	12.88 (0.00)
36	37.65 (0.00)	29.40 (0.00)	68.66 (0.00)	287.38 (0.00)	0.94 (0.00)	22.29 (0.00)
37	1063.09 (808.27)	2000.00	55.00	231.93	0.77	15.42
38	1063.09 (0.00)	1740.00 (0.00)	75.00 (0.00)	315.35 (0.00)	1.01 (0.00)	28.74 (0.00)
39	1063.09 (808.27)	1440.00	85.00	357.03	1.13	36.76
40	40.00 (0.00)	223.00 (0.00)	232.70 (0.00)	2935.65 (0.00)	7.59 (0.00)	786.94 (0.00)

Table 3
Performance indicator comparison at 100%THA load.

Item	Extraction flow rate (kg/s)	Original System	New System	Difference
Power output (MW)	10	127.07	127.44	0.37
	20	123.51	124.24	0.73
	30	119.94	121.04	1.10
	40	116.37	117.84	1.47
Heating capacity (kW)	10	25,460.54	33,487.20	8,026.66
	20	50,921.08	66,974.41	16,053.33
	30	76,381.63	100,461.61	24,079.98
	40	101,842.17	133,948.81	32,106.64
Coal consumption for power generation (g/kWh)	10	329.13	321.44	7.69
	20	317.37	303.29	14.08
	30	307.13	287.61	19.51
	40	298.20	273.98	24.22
Coal consumption for heating (kg/GJ)	10	32.06	31.50	0.56
	20	30.36	29.37	0.99
	30	28.83	27.51	1.32
	40	27.44	25.88	1.56
Integral thermal efficiency (%)	10	42.59	44.93	2.34
	20	48.71	53.39	4.68
	30	54.82	61.85	7.03
	40	60.93	70.31	9.38

$$\eta_{ex} = \frac{P_{integral} + Ex_{Qh}}{Ex_z} \tag{52}$$

where η_{th} and η_{ex} respectively denotes integral thermal and exergy efficiency, %;Ex_{Qh} and Ex_z respectively denotes exergy of heating capacity and integral exergy input into the system, kW.

4. Results and discussion

Based on the first and second laws of thermodynamics, the performance indicators and exergy indicators of the traditional cogeneration system and the new cogeneration system with ORC and AHP have been analyzed to comprehensively reveal the performance change at 100% THA, 75%THA and 50%THA load before and after transformation. The thermodynamic parameters are exhibited at 100%THA load in Table 2 in which values in parentheses are corresponding values of the traditional cogeneration system. The parameters outside parentheses represent thermodynamic parameters of integrated system with AHP and ORC, while the parameters inside parentheses represent thermodynamic parameters of traditional cogeneration system. The parameters without parentheses represent the same parameters in both systems. The performance indicator comparison is shown in Table 3 at 100%THA load and different heating extraction steam flow rates.

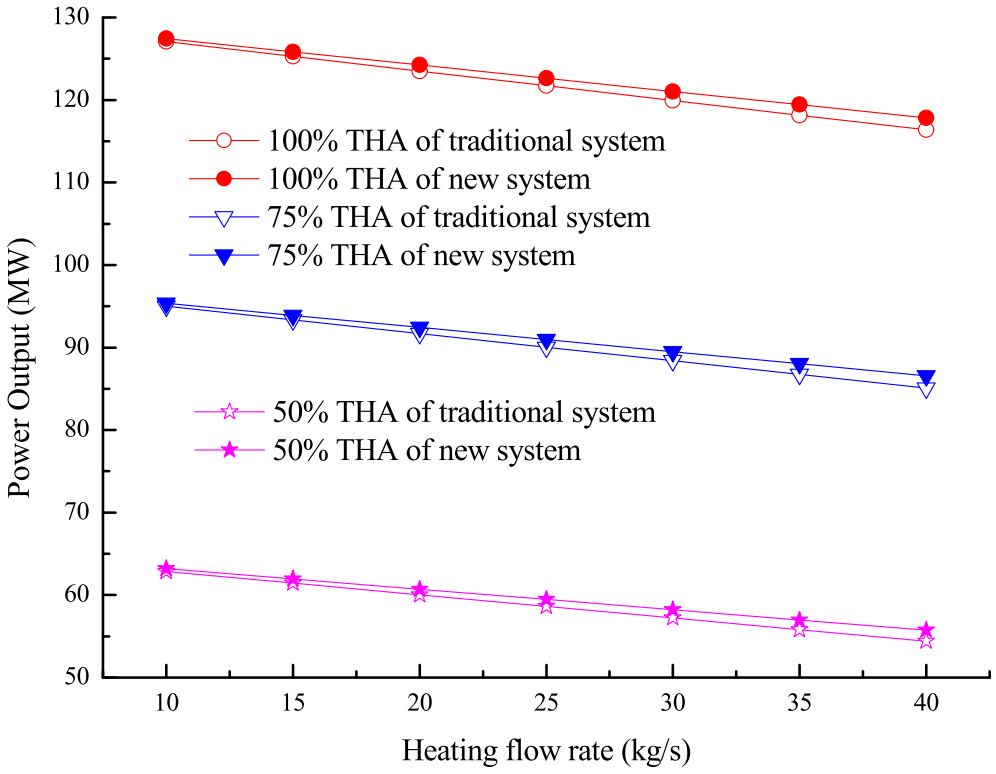

Fig. 6. Power output of original and new systems at different loads and extraction flow rates.

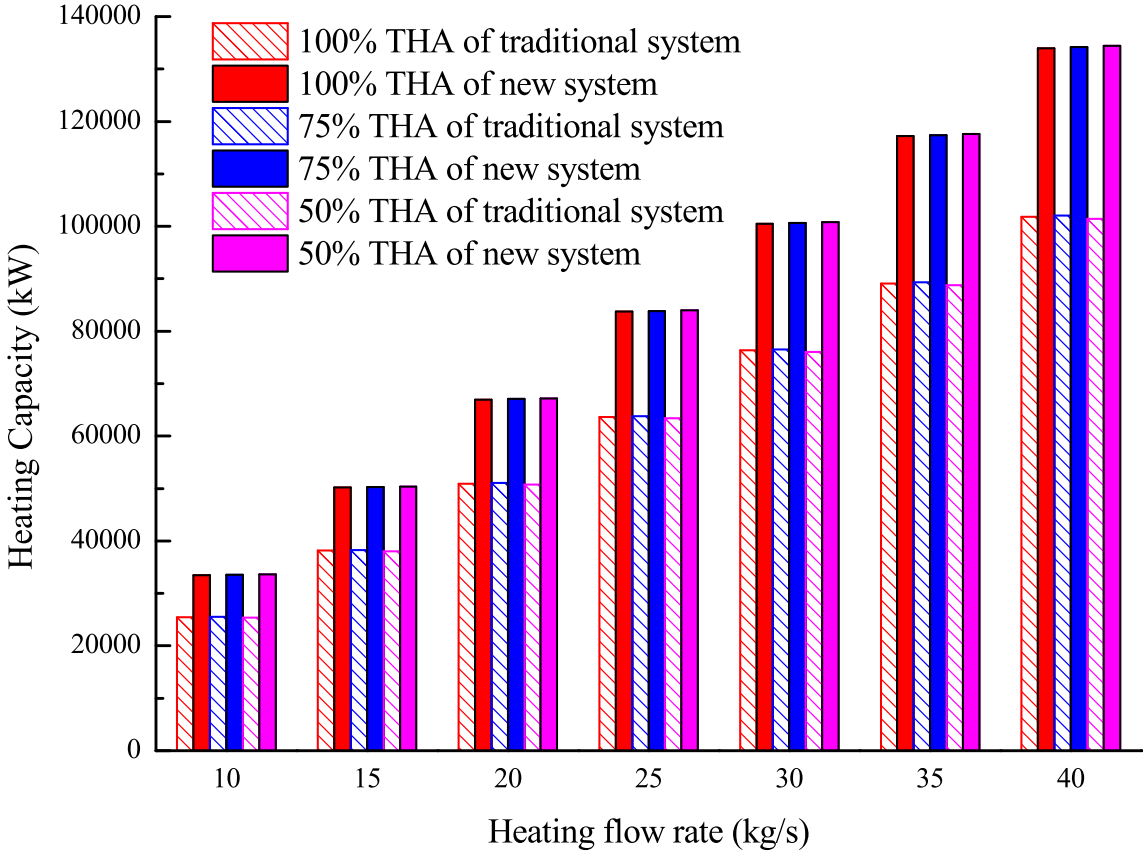

Fig. 7. Heating capacity of original and new systems at different loads and extraction flow rates.

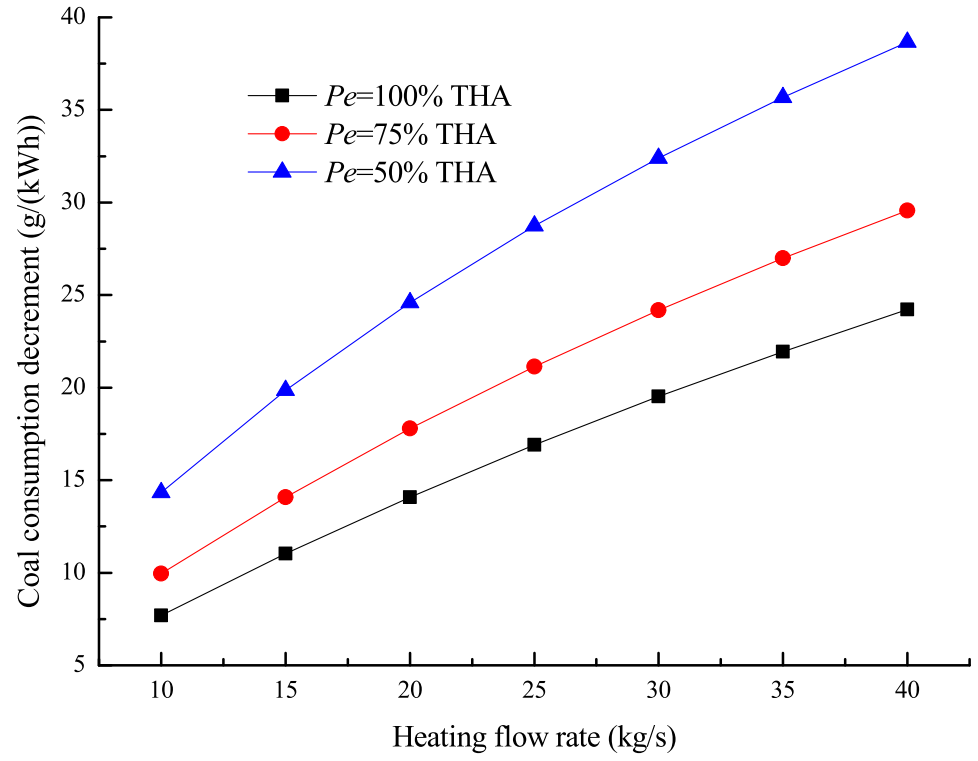

Fig. 8. Coal consumption decrement variation for power generation at different loads and extraction flow rates.

4.1. Performance indicator analyses

4.1.1. Power output

The power output variation of the two cogeneration system is illustrated in Fig. 6 at different loads and flow rates of heating extraction steam. As shown in Fig. 6, the power output of the cogeneration system with ORC and AHP is larger than that of traditional cogeneration system. The power increment augments with the increase of the flow rate of heating extraction steam at the same load. The power increment increases from 0.37 MW to 1.47 MW when the flow rate of heating

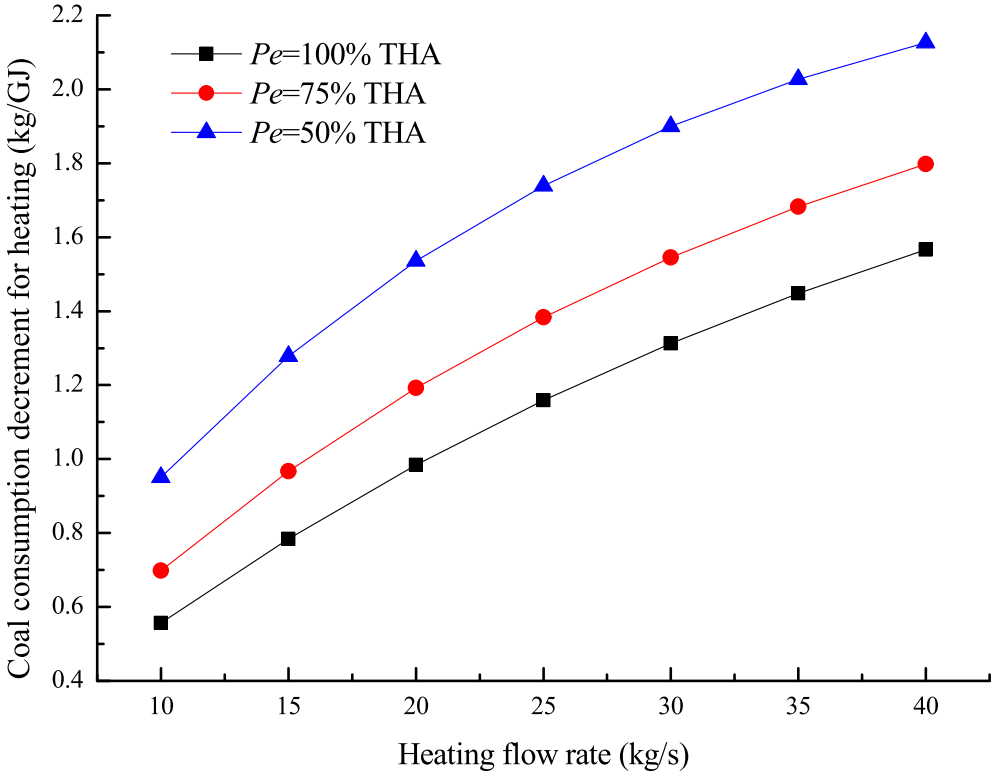

Fig. 9. Coal consumption decrement variation for heat-supplying at different loads and extraction flow rates.

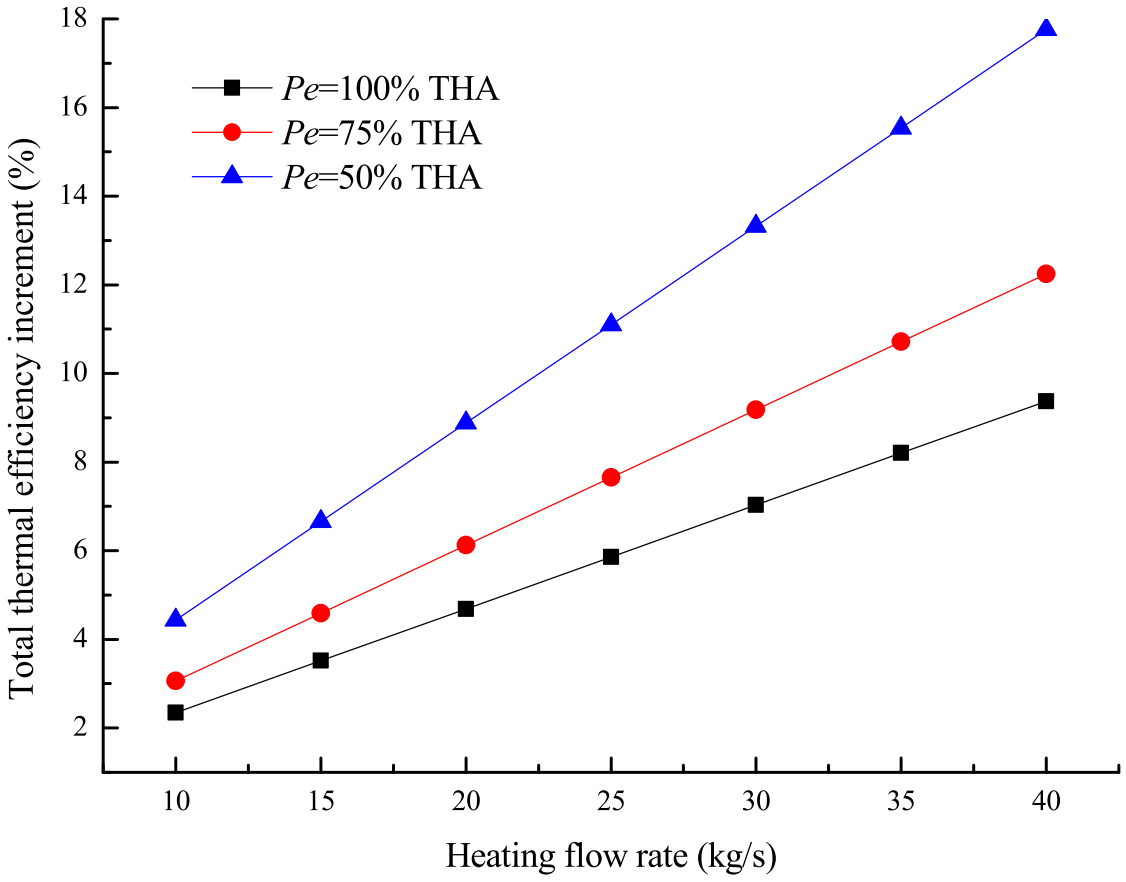

Fig. 10. Integral thermal efficiency increment variation at different loads and extraction flow rates.

extraction steam increase from 10 kg/s to 40 kg/s at 100% THA load. The reason is that the driving heat increases to increase power generation of ORC with increasing flow rate of heating extraction steam. Therefore, additional power can be obtained from the high-quality heating extraction steam in the new system, which improves the efficient utilization of high-quality heat energy.

4.1.2. Heating capacity

The heating capacity variation of the two cogeneration system is shown in Fig. 7 at different loads and flow rates of heating extraction steam.

The heating capacity of the cogeneration system with ORC and AHP is larger than that of traditional cogeneration system. It can be seen that the amount of heat provided for heating is decreased, but the heating capacity is increased in the new cogeneration system. The reason is that a part of waste heat from exhausted steam is recovered by AHP to supply heating, which uses low-grade heat energy for heating. The heating capacity increment augments with the increase of the flow rate of heating extraction steam at the same load. The heating capacity increment increases from 8,026.66 kW to 32,106.64 kW when the flow rate of heating extraction steam increases from 10 kg/s to 40 kg/s at 100% THA load. This phenomenon is caused by the increase of waste heat recovered by AHP with increasing extraction steam flow rate. It can be seen from Figs. 6 and 7 that the relatively high-quality heat energy is used to generate power and relatively low-quality heat energy is used to supply heat in the proposed cogeneration system, which can achieve the dual purposes of increasing power generation and heat supply.

4.1.3. Coal consumption for power generation

The coal consumption decrement variation for power generation of the two cogeneration system is exhibited in Fig. 8 at different loads and flow rates of heating extraction steam.

The coal consumption for power generation in the cogeneration system with ORC and AHP is significantly decreased compared with the traditional cogeneration system. The coal consumption decrement increases with the increase of flow rate of heating extraction steam at the same load. The coal consumption decrement increases from 7.69 g/(kWh) to 24.22 g/(kWh) when the flow rate of heating extraction steam increases from 10 kg/s to 40 kg/s at 100% THA load. It is due to the increase of power generation increment with increasing extraction flow rate. Moreover, the difference of coal consumption for power generation is more obvious at lower operating loads under the same heating extraction flow rate.

4.1.4. Coal consumption of heat-supplying

The coal consumption decrement variation for heat-supplying between the two cogeneration systems is shown in Fig. 9 at different loads and flow rates of heating extraction steam.

The coal consumption for heat-supplying in the cogeneration system with ORC and AHP is less than that of traditional cogeneration system. Compared with traditional cogeneration system, the coal consumption for heat-supplying reduces from 27.44 kg/GJ to 25.88 kg/GJ in the new system when the heating extraction flow rate is 40 kg/s. The reason is that a part of waste heat from exhausted steam is recovered by AHP to supply heating to increase the heating capacity. In addition, the coal consumption decrement for heat-supplying augments with increasing heating extraction flow rate and decreasing load. As can be seen from Figs. 8 and 9, the fuel consumption can be effectively saved in the proposed new cogeneration system.

4.1.5. Integral thermal efficiency

The integral thermal efficiency increment variation between the two

Table 4
Exergy analysis results of main facilities at 100%THA load when heating extraction flow rate is 40 kg/s.

Item		Traditional cogeneration system			New cogeneration system		
		Exergy loss(MW)	Exergy loss rate (%)	Exergy efficiency (%)	Exergy loss (MW)	Exergy loss rate (%)	Exergy efficiency (%)
ST	HPT	5.248	1.99	89.37	5.247	2.08	89.37
	IPT	3.762	1.43	94.09	3.761	1.49	94.09
	LPT	2.346	0.89	84.33	2.300	0.91	89.34
	Σ	11.355	4.31	91.59	11.308	4.48	91.60
RS	1#HPH	0.362	0.14	93.58	0.362	0.14	93.58
	2#HPH	1.434	0.54	88.80	1.434	0.57	88.80
	3#DH	0.400	0.15	93.37	0.400	0.16	93.37
	4#LPH	0.467	0.18	86.56	0.467	0.19	86.56
	5#LPH	0.433	0.16	88.04	0.588	0.23	84.33
	6#LPH	0.479	0.18	74.96	0.643	0.25	75.30
	Σ	3.575	1.35	93.52	3.894	1.54	90.57
Boiler	①	3.377	1.28	—	3.377	1.34	—
	②	0.675	0.26	—	0.675	0.27	—
	③	2.915	1.10	—	2.915	1.15	—
	④	3.092	1.17	—	3.092	1.22	—
	⑤	0.959	0.36	—	0.959	0.38	—
	⑥	143.889	54.49	—	143.889	56.90	—
	⑦	52.834	20.01	—	52.834	20.89	—
	Σ	207.742	78.67	47.63	207.742	82.15	47.63
ACC		28.863	10.93	2.52	18.565	7.34	5.20
AHP		0.000	0.00	0.00	5.549	2.19	71.86
HHN		12.519	4.74	57.94	4.228	1.67	66.83
ORC		0.000	0.00	0.00	1.600	0.63	49.62
Whole system		264.055	100.0	37.13	252.885	100.0	38.84

①smoke exhaust ②chemistry factor ③machinery factor ④heat dissipation ⑤boiler ash ⑥combustion ⑦heat transfer.

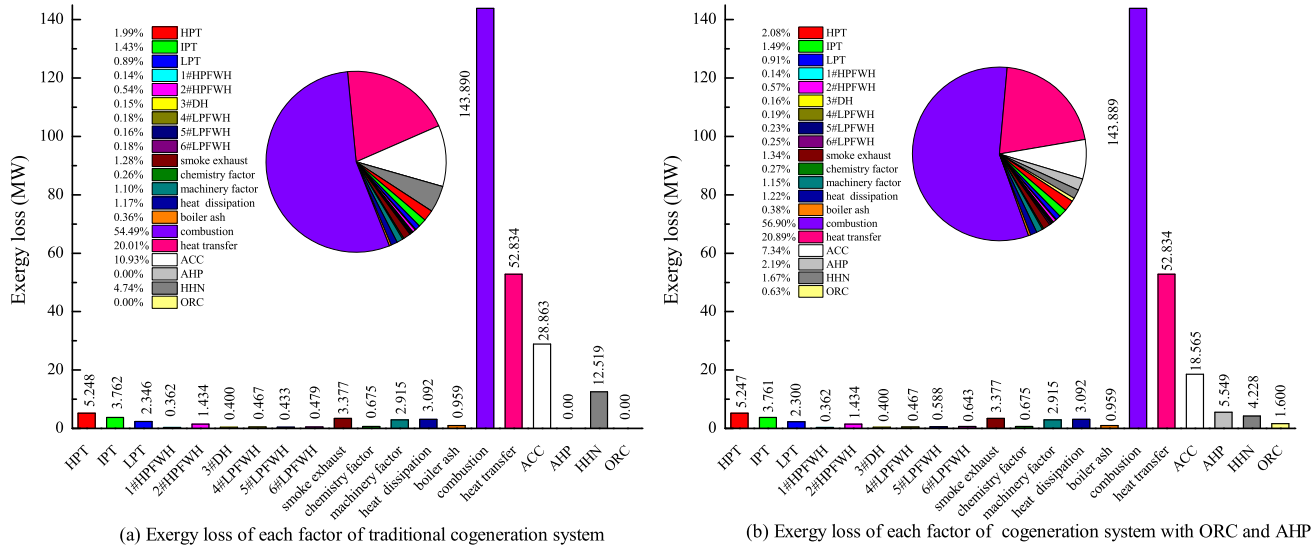

(a) Exergy loss of each factor of traditional cogeneration system

(b) Exergy loss of each factor of cogeneration system with ORC and AHP

Fig. 11. Exergy loss distribution of each factor at 100% THA.

cogeneration systems is presented in Fig. 10 at different loads and flow rates of heating extraction steam. The integral thermal efficiency of the cogeneration system with ORC and AHP is significantly higher than that of traditional cogeneration system. The integral thermal efficiency increment augments with the increase of flow rate of heating extraction steam at the same load. The integral thermal efficiency increment augments from 2.34% to 9.38% when the flow rate of heating extraction steam increases from 10 kg/s to 40 kg/s at 100%THA load. This is because the power generation and heating capacity both increase with increasing heating extraction flow rate. Moreover, the lower the load is, the more significant integral thermal efficiency increment is. Therefore, the thermal efficiency of the whole system can be significantly improved in the new cogeneration system.

4.2. Exergy analyses of the system

In order to reveal the efficient use of energy, the exergy analyses of the traditional cogeneration system and the new cogeneration system with ORC and AHP have been performed.

4.2.1. Exergy analyses under a specific condition

The exergy indicator calculated results of each factor in the two systems are listed in Table 4 at 100%THA when the flow rate of heating extraction steam is 40 kg/s. As can be seen from the Table, the integral exergy losses are respectively 264.055 MW and 252.885 MW, and integral exergy efficiencies are 37.13% and 38.84% in the two cogeneration system. Compared with traditional cogeneration system, integral exergy loss can be saved by 11.170 MW and integral exergy efficiency can be improved by 1.71% in the new cogneration system.

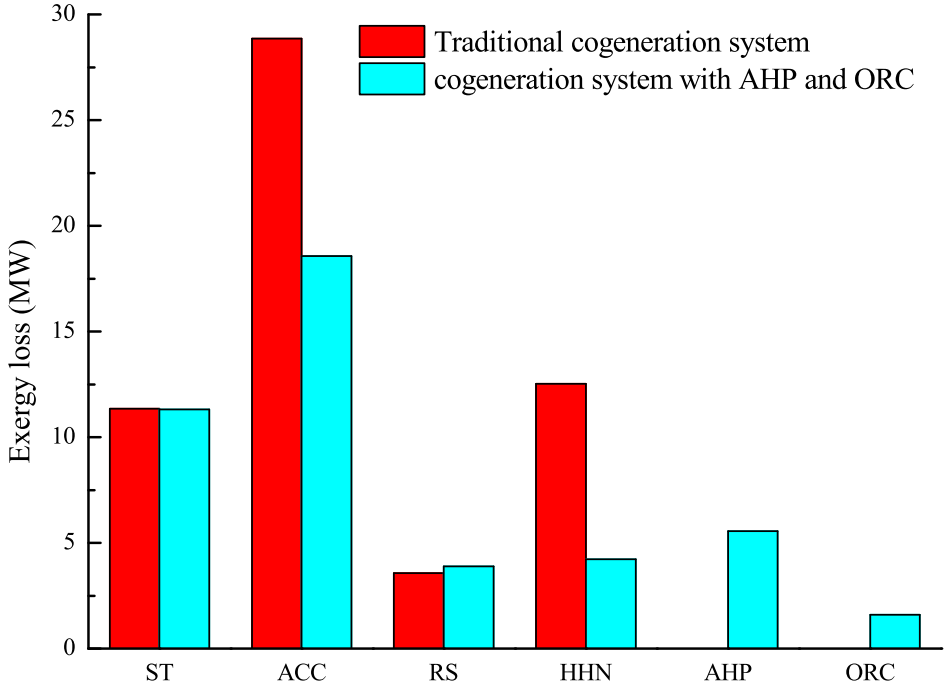

Fig. 12. Exergy loss distribution of each subsystem at 100% THA.

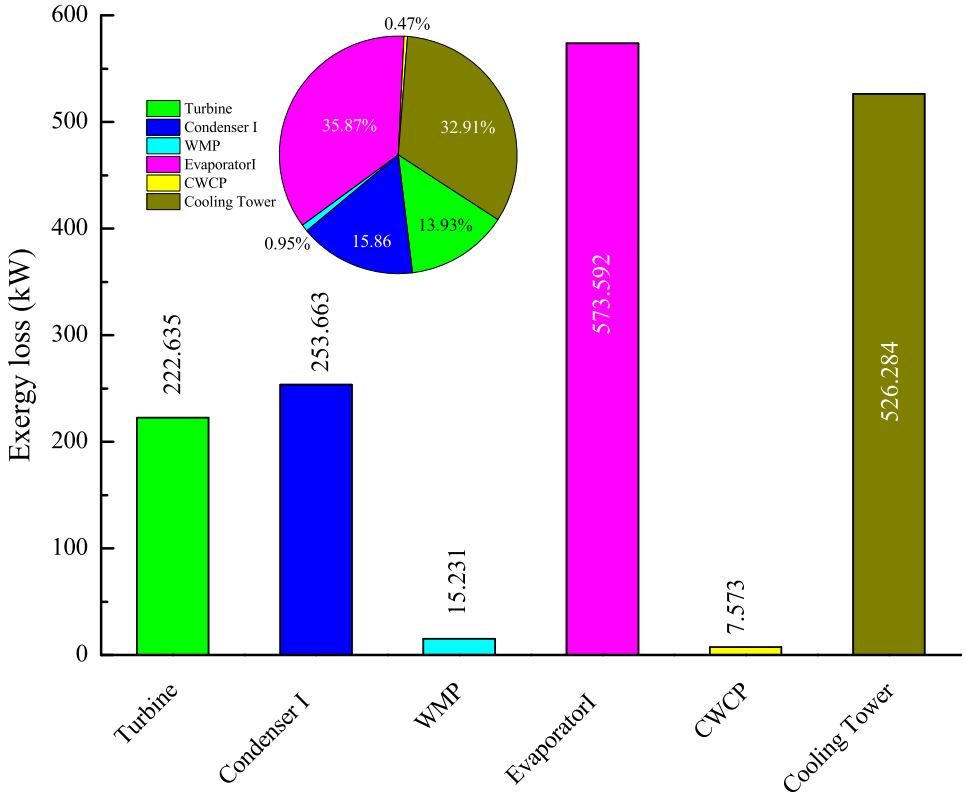

Fig. 13. Exergy loss distribution of ORC.

The exnergy loss distribution of each factor is exhibited in Fig. 11. As shown in Fig. 11, the exergy loss factors in the first three are successively boiler combustion, boiler heat transfer and air cooling condenser. Their exergy loss rates are respectively 54.49%, 20.01%, 10.93% and 56.90%, 20.89%, 7.34% in the two cogeneration systems. The exergy loss of each feed-water heater is relatively small, and the maximum exergy loss rate is no more than 0.6%. The exergy loss of each cylinder in the steam turbine does not vary greatly. Since the modification does not involve the boiler, the exergy loss of the boiler remains unchanged.

The exergy loss distribution of each subsystem at 100% THA is

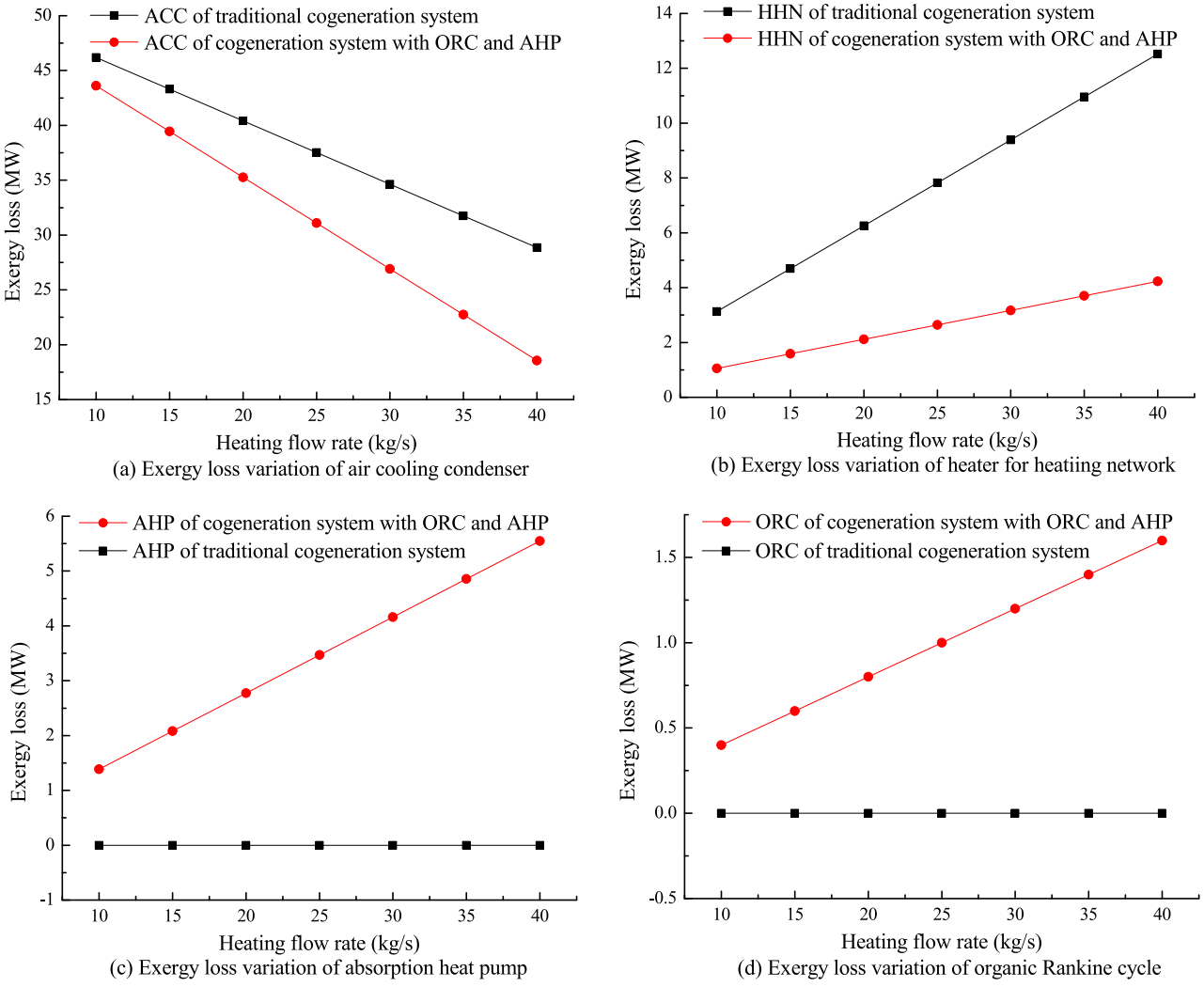

Fig. 14. Exergy losses of some subsystems at different heating extraction flow rates.

displayed in Fig. 12. After the modification, the exergy loss of the ST (steam turbine) system is slightly decreased, and that of the RS (regenerative system) is slightly increased. The added exergy losses caused by AHP and ORC are respectively 5.549 MW and 1.600 MW in the new system. However, the exergy losses of HHN and ACC are reduced from 12.519 MW to 4.228 MW and 28.863 MW to 18.565 MW, which respectively decreases by 8.291 MW and 10.298 MW. Compared with traditional cogeneration system, the exergy loss of AHP and ORC are added, but the exergy loss of HHN and ACC are greatly reduced in the cogeneration system with ORC and AHP. The reason is that the combined application of ORC and AHP reduces the irreversible loss of heat transfer in HHN and recovers waste heat from exhausted steam that should have been discharged into the ACC to be condensed.

The exergy loss distribution of ORC system is shown in Fig. 13. The exergy losses of evaporator I and cooling tower are relatively large and exergy loss rates account for 35.87% and 32.91%, respectively. It indicated that evaporator I and cooling tower are the most potential energy saving facilities in ORC system. The exergy loss can be reduced by reducing the heat transfer temperature difference of the evaporator I and recovering the waste heat of the cooling tower. The exergy loss of WMP (Working medium pump) and CWCP (Cooling water circulating pump) is relatively small and the exergy loss rates are 0.95% and 0.47%. The added exergy loss caused by the turbine is 222.635 kW, but additional power of 1435.589 kW generated by the trubine is obtained. The exergy efficiency of ORC system is 49.62%, which is much higer than that of the whole integrated system (see Table 4). It also shows that the ORC is more efficient for the utilizaton of medium- and low-temperature heat energy.

The exergy loss variations of some subsystems at different heating extraction flow rates are presented in Fig. 14. As can be seen from Fig. 14 (a), the exergy loss of air cooling condenser continuously reduces in the two cogeneration systems with increasing heating extraction flow rate. This is because the flow rate of exhausted steam from ST into air cooling condenser is reduced to decrease the exergy dissipation. As dispalyed in Fig. 14(b), the exergy loss of HHN increases with increasing heating extraction flow rate. This is due to exergy loss of heat transfer in HHN is increased with increasing heating capacity. As exhibited in Fig. 14(c) and (d), the exergy losses of AHP and ORC increases with increasing heating extraction flow rate in the new cogeneration system. Although the exergy losses of two subsystems both are increased, the waste heat recovery capacity of AHP and power generation capacity of ORC are also correspondingly improved.

4.2.2. Exergy analysis at different loads and heating extraction flow rates

The integral exergy loss variation of the two cogeneration systems at different loads and heating extraction flow rates is shown in Fig. 15. The integral exergy loss of the cogeneration system with ORC and AHP is less than that of traditional cogeneration system. Moreover, the integral

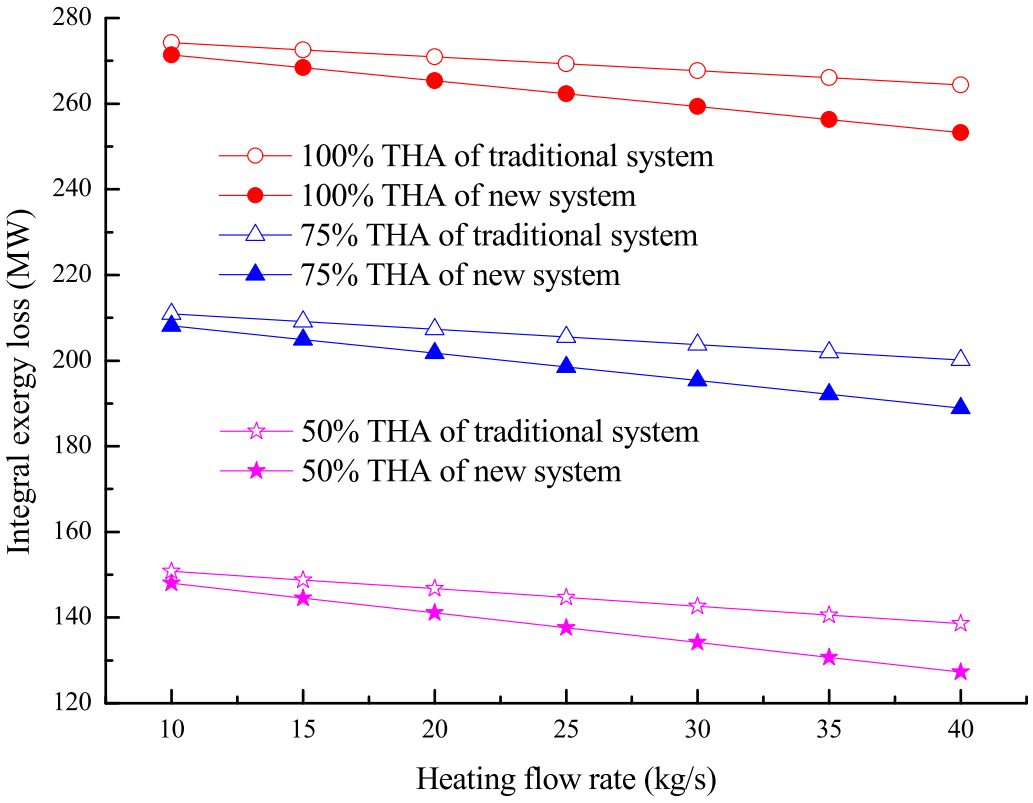

Fig. 15. Integral exergy loss at different loads and heating extraction flow rate.

Table 5
Integral exergy loss and efficiency at 100% THA at different heating extraction flow rates.

Item	Extraction flow rate (kg/s)	Original System	New System	Difference
Integral exergy loss (MW)	10	274.211	271.408	2.803
	20	270.952	265.353	5.599
	30	267.682	259.295	8.387
	40	264.395	253.235	11.160
Integral exergy efficiency (%)	10	36.87	37.30	0.43
	20	36.96	37.81	0.85
	30	37.04	38.33	1.29
	40	37.13	38.84	1.71

exergy loss decrement increases with the increasing flow rate of heating extraction steam at the same load. As shown in Fig. 15 and Table 5, the integral exergy loss decrement increases from 2.830 MW to 11.160 MW when the flow rate of heating extraction steam increases from 10 kg/s to 40 kg/s at 100% THA load. The reason is that the increment of heating capacity and power generation both increase due to combined application of ORC and AHP with increasing heating extraction flow rate in the new cogeneration.

As exhibited in Fig. 16, the integral exergy efficiency of the cogeneration system with ORC and AHP is significantly higher than that of traditional cogeneration system. The integral exergy efficiency increment augments with the increase of flow rate of heating extraction steam at the same load. The integral exergy efficiency increment augments from 0.43% to 1.71% when the flow rate of heating extraction steam increases from 10 kg/s to 40 kg/s at 100% THA load. The reason is that the power generation capacity of ORC and the waste heat recovery effect of AHP are both increased with increasing heating extraction flow rates. In addition, the lower the load is, the more significant integral exergy efficiency increment is. Therefore, the energy effective utilization of the whole system can be significantly improved in the new cogeneration system.

5. Conclusions

In the paper, a new cogeneration system based on ORC and AHP is proposed, and the performance analysis has been carried out in terms of first and second thermodynamic law. The result indicates that the dual purpose of increasing power output and heating capacity can be achieved in the new cogeneration system. Compared to traditional cogeneration system, the power output and heating capacity is increased by 0.37–1.47 MW and 8,026.66–32,106.64 kW at 100%THA load. The integral exergy loss is reduced by 2.803–11.160 MW. The coal consumption for power generation and heating-supply are both significantly reduced. The integral thermal and exergy efficiencies are improved by 2.34%-9.38% and 0.43%-1.71%. In addition, the integral thermal and exergy efficiency increment both augment with the increase of flow rate of heating extraction steam. Therefore, the proposed combined application of the ORC and AHP can not only improve the power output and heating capacity of the existing heat source in the cogeneration system but also save fuel consumption, which will bring great benefits to coal-fired power plants.

CRediT authorship contribution statement

Hongsheng Zhang: Conceptualization, Methodology, Software, Formal analysis, Writing - original draft, Writing - review & editing, Supervision. **Yifeng Liu:** Conceptualization, Investigation, Writing - review & editing, Visualization. **Xingang Liu:** Conceptualization, Investigation, Writing - review & editing, Visualization. **Chenghong Duan:** Validation, Resources, Data curation, Writing - review & editing, Project administration.

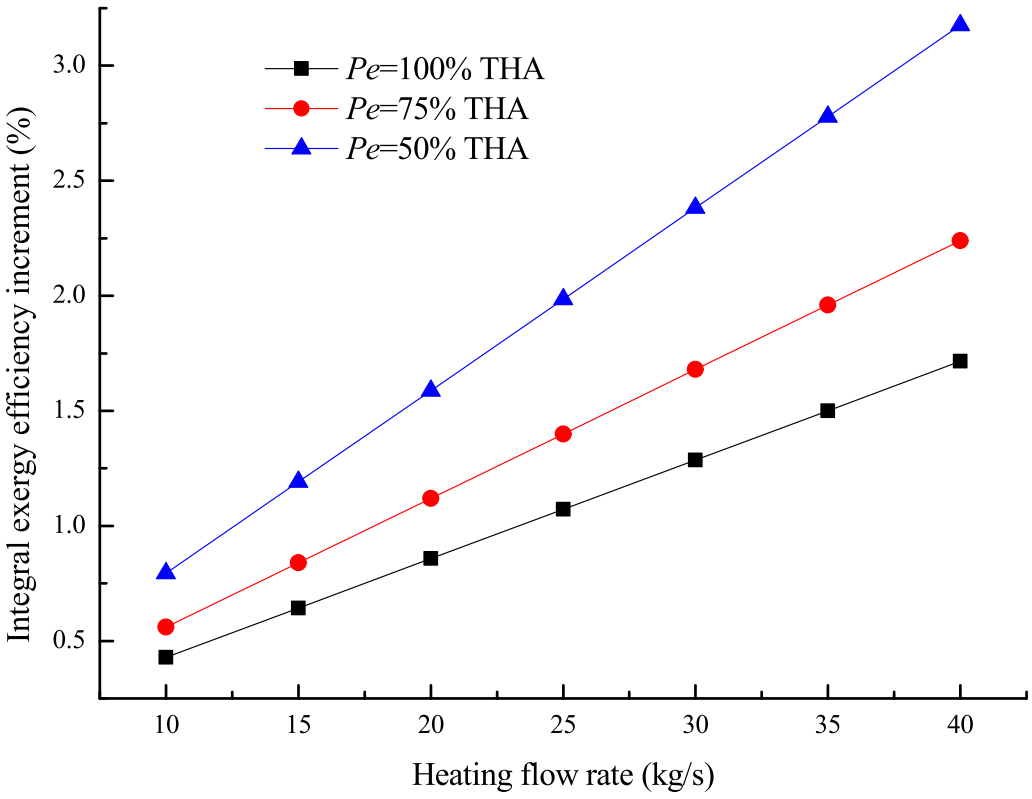

Fig. 16. Integral exergy efficiency increment at different loads and heating extraction flow rates.

Declaration of Competing Interest

The authors declare that they have no known competing financial interests or personal relationships that could have appeared to influence the work reported in this paper.

Acknowledgements

This project is supported by the Science Foundation of Beijing University of Chemical Technology, the Fundamental Research Funds for the Central Universities (BUCTRC202027) and the China Scholarship Council (CSC) (Grant No. 201706440092).

References

[1] Kwan TH, Katsushi F, Shen Y, Yin S, Zhang Y, Kase K, et al. Comprehensive review of integrating fuel cells to other energy systems for enhanced performance and enabling polygeneration. Renew Sustain Energy Rev 2020;128:109897.
[2] Bamati N, Raoofi A. Development level and the impact of technological factor on renewable energy production. Renew Energy 2020;151:946–55.
[3] Rullo P, Braccia L, Luppi P, Zumoffen D, Feroldi D. Integration of sizing and energy management based on economic predictive control for standalone hybrid renewable energy systems. Renew Energy 2019;140:436–51.
[4] Chen T, Shu G, Tian H, Zhao T, Zhang H, Zhang Z. Performance evaluation of metal-foam baffle exhaust heat exchanger for waste heat recovery. Appl Energy 2020;266:114875.
[5] Chu F, Su M, Yang G. Heat and mass transfer characteristics of ammonia regeneration in packed column. Appl Therm Eng 2020;176:115405.
[6] Vellini M, Gambini M, Stilo T. High-efficiency cogeneration systems for the food industry. J Cleaner Prod 2020;260:121133.
[7] Li W, Tian X, Li Y, Ma Y, Fu L. Combined heating operation optimization of the novel cogeneration system with multi turbine units. Energy Convers Manage 2018; 171:518–27.
[8] Zhao S, Ge Z, He J, Wang C, Yang Y, Li P. A novel mechanism for exhaust steam waste heat recovery in combined heat and power unit. Appl Energy 2017;204: 596–606.
[9] Dogbe ES, Mandegari M, Görgens JF. Assessment of the thermodynamic performance improvement of a typical sugar mill through the integration of waste-heat recovery technologies. Appl Therm Eng 2019;158:113768.
[10] Li X, Wang Z, Yang M, Yuan G. Modeling and simulation of a novel combined heat and power system with absorption heat pump based on solar thermal power tower plant. Energy 2019;186:115842.
[11] Li X, Wang Z, Yang M, Bai Y, Yuan G. Proposal and performance analysis of solar cogeneration system coupled with absorption heat pump. Appl Therm Eng 2019; 159:113873.
[12] Sun F, Fu L, Sun J, Zhang S. A new waste heat district heating system with combined heat and power (CHP) based on ejector heat exchangers and absorption heat pumps. Energy 2014;69:516–24.
[13] Zhang H, Li Z, Zhao H. Thermodynamic performance analysis of a novel electricity-heating cogeneration system (EHCS) based on absorption heat pump applied in the coal-fired power plant. Energy Convers Manage 2015;105:1125–37.
[14] Zhang H, Zhao H, Li Z. Waste heat recovery and water-saving modification for a water-cooled gas-steam combined cycle cogeneration system with absorption heat pump. Energy Convers Manage 2019;180:1129–38.
[15] Xu ZY, Mao HC, Liu DS, Wang RZ. Waste heat recovery of power plant with large scale serial absorption heat pumps. Energy 2018;165:1097–105.
[16] Li Y, An H, Li W, Zhang S, Jia X, Fu L. Thermodynamic, energy consumption and economic analyses of the novel cogeneration heating system based on condensed waste heat recovery. Energy Convers Manage 2018;177:671–81.
[17] Liao G, E J, Zhang F, Chen J, Leng E. Advanced exergy analysis for Organic Rankine Cycle-based layout to recover waste heat of flue gas. Appl Energy 2020; 266: 114891.
[18] Campos GB, Bringhenti C, Traverso A, Tomita JT. Thermoeconomic optimization of organic Rankine bottoming cycles for micro gas turbines. Appl Therm Eng 2020; 164:114477.
[19] Linnemann M, Priebe KP, Heim A, Wolff C, Vrabec J. Experimental investigation of a cascaded organic Rankine cycle plant for the utilization of waste heat at high and low temperature levels. Energy Convers Manage 2020;205:112381.
[20] Moreira LF, Arrieta FRP. Thermal and economic assessment of organic Rankine cycles for waste heat recovery in cement plants. Renew Sustain Energy Rev 2019; 114:109315.
[21] Bălănescu D, Homutescu V. Performance analysis of a gas turbine combined cycle power plant with waste heat recovery in Organic Rankine Cycle. Proc Manuf 2019; 32:520–8.
[22] Li H, Gu K, Ma C. Working fluids selection for heat source in different temperature ranges. Turbine Technol 2013;55(4):251–4 (in Chinese).
[23] Zhang HS, Zhao HB, Li ZL. Performance analysis of the coal-fired power plant with combined heat and power (CHP) based on absorption heat pumps. J Energy Inst 2016;89:70–80.
[24] Wu J, Hou H, Hu E, Yang Y. Performance improvement of coal-fired power generation system integrating solar to preheat feedwater and reheated steam. Sol Energy 2018;163:461–70.

[25] Song J, Li X, Ren X, Gu C. Performance analysis and parametric optimization of supercritical carbon dioxide (S-CO_2) cycle with bottoming Organic Rankine Cycle (ORC). Energy 2018;143:406–16.
[26] Liu G, Qin Y, Wang J, Liu C, Yin Y, Zhao J, et al. Thermodynamic modeling and analysis of a novel PEMFC-ORC combined power system. Energy Convers Manage 2020;217:112998.
[27] Keinath CM, Garimella S. Development and demonstration of a microscale absorption heat pump water heater. Int J Refrig 2018;88:151–71.
[28] Sa W. The research and application of type I lithium bromide absorption heat pump. Contam Control Air-Condition Technol 2010;2:21–4 (in Chinese).
[29] Li Y, Fu L, Zhang S, Zhao X. A new type of district heating system based on distributed absorption heat pumps. Energy 2011;36:4570–6.
[30] Abrahamsson K, Stenström S, Jernqvist G. Applicatoin of heat pump systems for energy conservation in paper drying. Int J Energy Res 1997;21:631–42.
[31] Zhang H, Zhao H, Li Z. Thermodynamic performance study on solar-assisted absorption heat pump cogeneration system in the coal-fired power plant. Energy 2016;116:942–55.
[32] Oyekale J, Petrollese M, Cau G. Modified auxiliary exergy costing in advanced exergoeconomic analysis applied to a hybrid solar-biomass organic Rankine cycle plant. Appl Energy 2020;268:114888.
[33] Ifaei P, Safder U, Yoo C. Multi-scale smart management of integrated energy systems, Part 1: energy, economic, environmental, exergy, risk (4ER) and water-exergy nexus analyses. Energy Convers Manage 2019;197:111851.